Two-Dimensional Superconducting Fluctuations Associated with Charge-Density-Wave Stripes in $La_{1.87}Sr_{0.13}Cu_{0.99}Fe_{0.01}O_4$

H. Huang,[1] S.-J. Lee ⬤,[1] Y. Ikeda,[2] T. Taniguchi,[2] M. Takahama,[2] C.-C. Kao,[3] M. Fujita,[2,*] and J.-S. Lee ⬤[1,†]

[1]*Stanford Synchrotron Radiation Lightsource, SLAC National Accelerator Laboratory, Menlo Park, California 94025, USA*
[2]*Institute for Materials Research, Tohoku University, Katahira 2-1-1, Sendai 980-8577, Japan*
[3]*SLAC National Accelerator Laboratory, Menlo Park, California 94025, USA*

The presence of a small concentration of in-plane Fe dopants in $La_{1.87}Sr_{0.13}Cu_{0.99}Fe_{0.01}O_4$ is known to enhance stripelike spin and charge density wave (SDW and CDW) order and suppress the superconducting T_c. Here, we show that it also induces highly two-dimensional superconducting correlations that have been argued to be the signatures of a new form of superconducting order, the so-called pair density wave (PDW) order. In addition, using resonant soft x-ray scattering, we find that the two-dimensional superconducting fluctuation is strongly associated with the CDW stripe. In particular, the PDW signature first appears when the correlation length of the CDW stripe grows over eight times the lattice unit ($\sim 8a$). These results provide critical conditions for the formation of the PDW order.

It has been more than 30 years since high-temperature superconductivity (HTSC) was discovered in 1986 [1]. Although tremendous progress has been made in understanding the fundamental mechanism of HTSC, especially in the high-T_c cuprates, the complexity of their phase diagrams [2] has complicated the problem; hence, there still remain many open issues. Some of the remaining profound questions are these: Why is the superconducting transition temperature (T_c) so high? How are different electronic and magnetic orders intertwined with HTSC? What is the pseudogap and how is it related to HTSC? Another interesting concern is the existence and characteristics of a possible new form of pairing, the so-called pair density wave (PDW), that potentially intertwines with several of the complex orders observed in the high-T_c cuprates [3]. Indeed, it has even been suggested that a fluctuating version of a PDW may be responsible for the famous pseudogap phenomenology [4–8].

In 2007, Li *et al.* [9] reported the existence of two-dimensional (2D) superconductivity in a high-T_c cuprate: $La_{1.875}Ba_{0.125}CuO_4$ (LBCO). This result, which is closely related but less clear-cut results of Tajima *et al.* [10], have been identified as signatures of the PDW order [11,12]. The most dramatic evidence of this unusual superconducting order is the existence of a range of temperatures, $T_c \approx 4$ K $< T < T_2 \approx 17$ K, in which the system exhibits an apparently anisotropic superconducting state. Specifically, in this temperature range, despite the existence of sufficiently strong 2D superconducting correlations such that the resistivity with the current flowing in the CuO_2 planes is immeasurably small, interlayer Josephson coupling is apparently absent, i.e., the c axis resistivity remains large. Here T_c is the transition temperature to the true

superconducting (Meissner) state. Furthermore, in a somewhat higher range of temperatures, $T_2 < T < T_1$, a fluctuating version of the same state, with an in-plane resistivity one or more orders of magnitude smaller than the normal state resistivity, onsets below a temperature, T_1, which is approximately equal to $T_{sdw} \approx 40$ K [13,14], the onset temperature of the spin density wave (SDW) stripe order in the CuO_2 planes. Since the charge density wave (CDW) stripe develops at a still higher temperature, ≈ 54 K [15–18], and thus coexists with the SDW at 40 K [14], it was suggested that this PDW signature originates from an intertwining of the HTSC, SDW, and CDW orders [3]. However, although the correlation between the SDW and CDW has been observed in multiple x-ray scattering measurements [14–18], no direct experimental evidence has unambiguously supported the association of this with the PDW order.

More recently, STM experiments in the halo region surrounding the vortex cores of $Bi_2Sr_2CaCu_2O_{8+\delta}$ (Bi2212) were performed by Edkins *et al.* [19], aimed to detect the field induced PDW. Through enhanced real- and Q-space resolutions in the STM, they revealed a CDW with a period approximately eight times the lattice unit ($\sim 8a$), twice that of the normal CDW period ($\sim 4a$). This observation is also thought to be a signature of a PDW. More detailed comparisons between microscopic theory and STM results have provided additional support for the existence of the PDW order in Bi2212 [20–22]. However, the observation of the PDW order through STM in Bi2212 is distinct from that in the LBCO system, if for no other reason than there is presently no evidence of any role of the SDW in the Bi2212 case. Although (the rather short-range correlated) CDW order coexists with the

superconducting phase of Bi2212 [23,24], it does not have a phase overlapping with the magnetic order in the phase diagram [25,26].

In this Letter, we explore new evidence of the putative PDW signature and its relation to other orders such as the CDW and SDW in an La-based high-T_c cuprate $La_{1.87}Sr_{0.13}Cu_{0.99}Fe_{0.01}O_4$ (LSCFO) [27]. It is important to stress that the crystal structure [28] of the LSCFO material [i.e., the low temperature orthorhombic (LTO) structure] is different from that of LBCO [i.e., the low temperature tetragonal (LTT) structure]. The LTT structure is known to suppress T_c and enhance the SDW and CDW orders [15–18,28]. In the present case, the CDW and SDW correlations are instead "pinned," and T_c is reduced by Fe doping rather than by the LTT structure. The pinned behavior is demonstrated by both the integrated intensity and peak position of the CDW with the development of the SDW. For this study, we carried out both transport measurements and resonant soft x-ray scattering (RSXS) around the Cu L_3 edge. Through the resistivity measurements along both the crystalline ab axis (i.e., the CuO_2 plane) and the c axis and the comparison between them, we have identified a state of 2D superconducting fluctuations that develops below $T_1 \approx 32$ K. The RSXS measurement revealed that the CDW short-range order (CDW-SRO) transforms into the CDW stripes with the development of SDW stripes below $T_{sdw} \approx 50$ K. In contrast to the case in LBCO, T_{sdw} is significantly larger than T_1, although the onset of the SDW order is visibly rounded and becomes notably sharper around T_1. We further observed that the correlation length of the CDW stripe reaches around $8a$ as the normal state undergoes a crossover to the 2D fluctuating state. While we do not observe any apparent vanishing of the in-plane resistivity at a temperature $T_1 > T_c \sim 5.7$ K [29,30], we do see a form of crossover (discussed below) that is in some ways analogous to T_1 in LBCO. In short, the similarities with the observed relations between the different ordering phenomena in the present system strongly corroborate the intertwined character of the different orders and, correspondingly, its association with PDW formation.

A sizable LSCFO single crystal was grown by the standard floating-solvent traveling-zone method. The grown crystal was annealed in one bar of O_2 gas to minimize oxygen deficiencies. The doped Fe ions are in the Fe^{3+} state ($3d^5$, $S = 5/2$), which have higher valence state than the Cu atoms by one, resulting in a reduction of one hole per doped ion. Thus, the concentration of hole (i.e., doping, p) in our LSCFO is 0.12. We confirm that this crystal does not undergo the LTT by temperature dependence of the (0 1 0) Bragg peak [30].

We first measured the resistivity (ρ) of our sample aiming to explore a PDW signature in LSCFO [27,31]. This measurement was motivated by the fact that the PDW order was observed in LBCO [9] and that La-based cuprates share the same mutual relationship between the
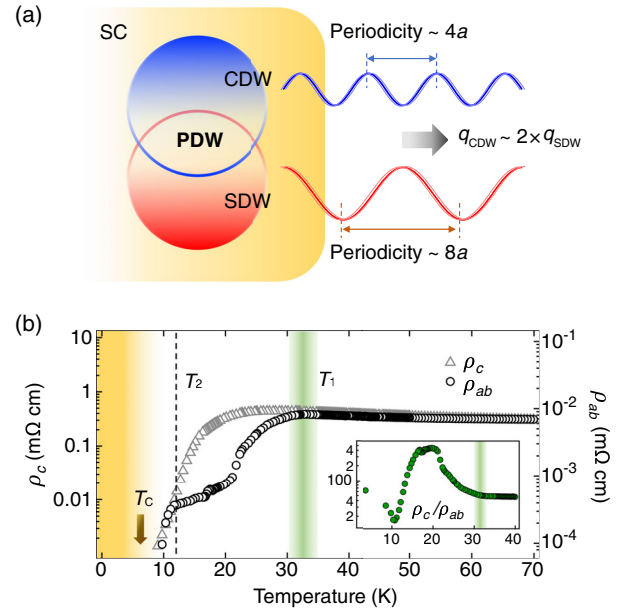

FIG. 1. (a) A schematic diagram of CDW and SDW stripes and their intertwining that results in the PDW order, implying the importance of their respective modulation phases. (b) Temperature dependence of the zero-field resistivity. ρ_c is along the c axis, and ρ_{ab} is parallel to the CuO_2 planes. The green shade and dashed line denote the first and second transitions in ρ_{ab}, respectively, above the Meissner state of both ρ_{ab} and ρ_c ($T_c \sim 5.7$ K). The inset shows the ratio of ρ_c to ρ_{ab} as a function of temperature.

CDW and SDW orders [14,18,30,32,33]. As illustrated in Fig. 1(a), it is well known that the ordering q vectors of the CDW and SDW orders (q_{cdw} and q_{sdw}) are related by $q_{cdw} \sim 2 \times q_{sdw}$ [32,33]. It was demonstrated that the LSCFO system also follows this relation [30]. Figure 1(b) shows the resistivity along the c axis (ρ_c) as well as that parallel to the CuO_2 plane (ρ_{ab}), which reveals an anisotropic behavior occurring around 32 K (T_1). Below the T_1, the value of ρ_{ab} gets as low as $\sim 10^{-3}$ mΩ cm, while $\rho_c \sim 10^0$ mΩ cm slightly increases. The anisotropy is even more obvious in the ρ_c/ρ_{ab} ratio plot (see the inset), showing an increase of 1 order of magnitude. This result shows a strong resemblance to the resistivity behavior in LBCO [9] and Zn-doped LBCO [34], leading to an interpretation that our LSCFO sample exhibits 2D fluctuating superconductivity (i.e., PDW fluctuation) around T_1. Note that we also observed magnetic field dependent ρ_{ab} [27]. A second drop of ρ_{ab} occurs around 11 K (T_2), deducing that the PDW fluctuation may change to a pure 2D superconducting state. Note that T_2 is still higher than the bulk $T_c \sim 5.7$ K of LSCFO [27].

Based on the observation of PDW fluctuation in the LSCFO, as a next step we investigated a relationship of the PDW fluctuation with the CDW and SDW orders in our sample. We measured the SDW order using the elastic
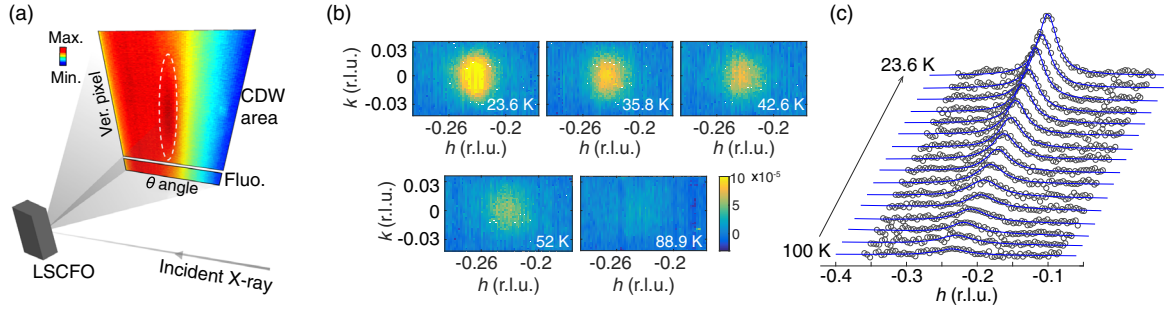
FIG. 2. (a) A schematic sketch showing the RSXS experiment on LSCFO using an area detector (CCD). At the fixed CCD angle (150°), θ scans were performed. The CDW signal is aligned on the center of the CCD detector. The bottom edge area of the image is regarded as the fluorescence (Fluo.) background-dominated region. (b) RSXS patterns in the h and k spaces of LSCFO for various sample temperatures after subtracting the fluorescence background. The CDW patterns are centered at $q_{cdw} \sim (-0.233, 0, l)$. Below ~ 50 K, the pattern tends to elongate along the k direction. (c) Projected scattering profiles along the h direction as a function of temperature. The solid lines are Lorentzian fits.

neutron scattering reported in Ref. [30]. For CDW measurements, we employed the RSXS approach, which has been demonstrated to detect small changes in weak CDW signals [15,33,35,36].

Figure 2(a) shows a schematic configuration for the RSXS measurements, where scattered x-ray signals were measured as a function of sample angle (θ) by a CCD detector. During the θ scan, the detector image covers scattering intensities from the well-aligned scattering plane (h, 0, l) near the detector center, as well as from the off-scattering planes (h, $\pm k$, l) at the top and bottom areas of the CCD. As depicted in the figure, we used the bottom part of the CCD images to subtract out the fluorescence background signal. After the background subtraction, we achieved clear CDW maps along the h and k directions centered at $q_{cdw} \sim (-0.23, 0, l)$ reciprocal lattice units (r.l.u.) [see Fig. 2(b) for the background-subtracted scattering maps at selected temperatures]. As shown in the figure, the CDW peaks are elongated along the k direction as the temperature is decreased below $T_{sdw} \sim 50$ K. This observation is consistent with previous reports on $La_{2-x}Sr_xCuO_4$ (LSCO) where CDW signals showed peak splitting through intertwining between the CDW and SDW stripes [33,36,37], suggesting that the CDW stripes are also formed in LSCFO. Figure 2(c) shows projected CDW signals along the h direction as a function of temperature. We fitted the projected CDW peaks with the Lorentzian function (blue lines in this figure), and the results are summarized in Fig. 3.

Similarly to the LSCO case [33], the CDW order in LSCFO continuously develops as the sample is cooled down from above 120 K. As shown in Fig. 3(a), the integrated intensity (left y axis) of the CDW peak keeps growing with decreasing temperature. Notably, the growing trend shows a change around 50 K, indicating a transition of the CDW. Note that the transition behavior is not sharp because the characteristics of density wave orders are

typically glassy in the cuprates. The high temperature CDW-SRO phase is transformed into the CDW stripe around this temperature, as was the case for LSCO [33]. Furthermore, this slope change in the integrated intensity coincides with a slope change in the wave vector of the CDW order (q_{cdw}, right y axis). The q_{cdw} decreases with decreasing temperature but is locked in below 50 K. Considering the LBCO case [18], this locking in
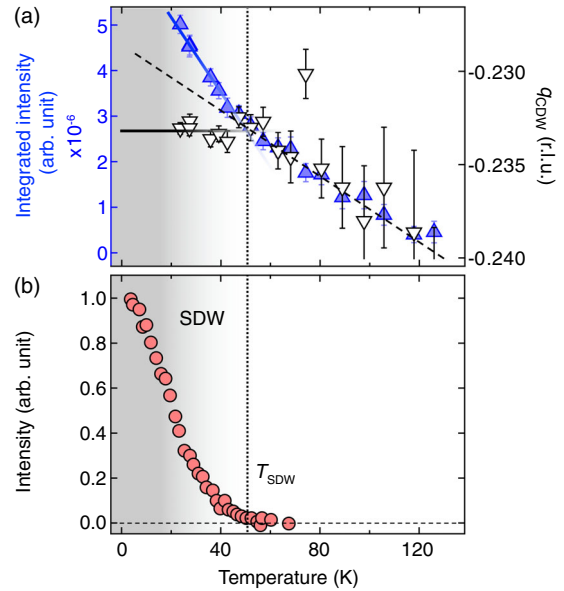

FIG. 3. (a) Integrated intensity (up triangles) of the CDW order (left y axis) and its wave vector q_{cdw} (down triangles, right y axis) as a function of temperature. Below ~ 50 K (denoted by the vertical dotted line), both the intensity and the q_{cdw} incommensurability show a different trend. The error bars represent 1 standard deviation of the fit parameters. (b) Temperature dependence of the SDW peak intensity measured by elastic neutron scattering. The SDW data was taken from Ref. [30]. The vertical dotted line at ~ 50 K denotes the onset of the SDW order.
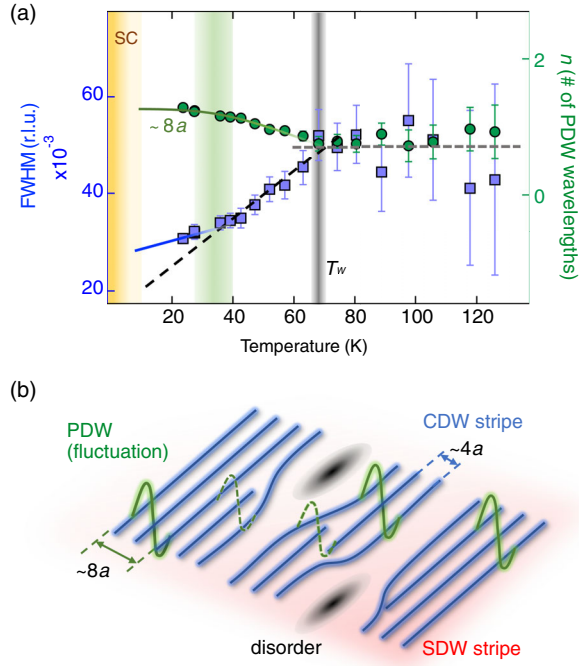
FIG. 4. (a) FWHM (squares) of the CDW order (left y axis) and the number of wavelengths (circles) for the PDW order (right y axis). The number of wavelengths (n) is estimated by $\xi_{CDW}/8a$, where ξ_{CDW} is calculated as 2/FWHM. Note that the FWHM and n show the same trend because they are inversely proportional to each other; they are plotted with the different axis scales. The vertical gray shade denotes a characteristic temperature (T_w) at which the FWHM of CDW starts to change while cooling down. The vertical green shade denotes another slope change in FWHM that is close to the first anisotropic transition (T_1) in ρ_{ab}. Below $T_1 \sim 32$ K, n is larger than 1. (b) A schematic diagram of a CuO_2 plane in LSCFO illustrating the formation of the PDW order. The PDW (fluctuation) starts to form when the domain size of CDW is over $\sim 8a$. The dashed green curves represent a situation where the PDW cannot be formed because of insufficient ξ_{CDW}. The black shades denote intrinsic disorders.

LSCFO can be explained by the development of the SDW stripe. As shown in Fig. 3(b), 50 K is the temperature where the SDW stripe develops [30]. These results indicate that the CDW stripe phase is developed by intertwining with the SDW. However, the discrepancy between this intertwining temperature and the onset temperature of the PDW fluctuation obtained by the transport measurement [Fig. 1(b)] calls for explanation.

To understand the discrepancy, we further scrutinize the CDW correlation lengths (ξ_{CDW}) in LSCFO. Figure 4(a) shows the full width at half maximum (FWHM) of the CDW peak as a function of temperature (left y axis). For $T > 70$ K, the FWHM does not change within the error, representing a T-independent region. This T-independent FWHM corresponds to $\xi_{CDW} \sim 23(2)$ Å, which is longer than the CDW wavelength, $\xi_{CDW} \sim 4a \sim 15$ Å. For $T < 70$ K, on the other hand, the FWHM starts to decrease

(ξ_{CDW} increases) with decreasing temperature. Following the discussion in Ref. [33], we assign 70 K to the characteristic temperature (T_w).

The FWHM behavior shows another noteworthy feature. The increasing trend of ξ_{CDW} below the T_w appears to undergo another slope change around 34 ± 3 K [27], which is close to the crossover temperature (T_1) of the PDW fluctuating states. A very interesting observation is that the measured ξ_{CDW} at this temperature is around 35(2) Å, which is close to the PDW wavelength, $\lambda_{PDW} \sim 8a \sim 30$ Å. For easier comparison between the two wavelengths, we plotted the ratio $n = \xi_{CDW}/\lambda_{PDW}$ on the right y axis in Fig. 4(a). At T_1, n is slightly over one. This observation implies that $\xi_{CDW} \geq \lambda_{PDW}$ is a critical condition, together with the presence of the CDW stripe, for the formation of the PDW order, as highlighted in Fig. 4(b). When the domain size of the CDW stripe is smaller than $8a$, PDW fluctuation cannot be formed [green dashed line in Fig. 4(b)] even when both the SDW and CDW are present. These conditions are fully compatible with the LBCO case, where the PDW was readily formed when CDW stripes were formed around the SDW temperature [9], because at this temperature the ξ_{CDW} is fairly long and already meets the $\xi_{CDW} \geq \lambda_{PDW}$ condition due to the LTT [14,17].

We now discuss the implications of our findings. First, the new evidence of the 2D superconducting signature in this LSCFO system means the PDW order observed in LBCO is not a consequence of some material science specific to LBCO but could be ubiquitous in La-based cuprates. Second, our findings, especially the critical prerequisite conditions for the PDW, are compatible with the two PDW (or its fluctuation) signatures observed in LBCO and Bi2212 [9,19,38], which seemingly contradict each other. Considering the enhancement of ξ_{CDW} below T_c under the magnetic field as a result of the well-known competition between the CDW and SC orders [39–41], the vortex halo region in Bi2212 under the magnetic field is expected to have a large CDW domain size, satisfying the correlation length condition to trigger the PDW. In La-based cuprates, this condition is met by a different mechanism; the SDW stripe order helps develop a long-ranged CDW stripe through intertwining. The different situations of Bi2212 and La-based cuprates lead to another critical implication that, of the two orders, namely the CDW and SDW stripes, the CDW stripe (or ξ_{CDW}) is the more essential ingredient for prompting the PDW. This implication is also supported by the observation that, for LSCO with 10% hole doping, the measured c-axis superconducting coherence is abruptly quenched with a magnetic field (smaller than H_{c2}) while the same magnetic field strongly enhances the stripe order [42,43]. Finally, one may extend the implications to a broader context of the pseudogap phenomenology in the high-T_c cuprates [4–8]. There are some pieces of evidence on the unusual gap features that suggest a PDW fluctuation

may be responsible for the pseudogap phenomenology [5–8]. Nevertheless, due to the different energy and temperature scales of these two phenomena, it is still too early to connect them directly. On the other hand, we may contemplate that the CDW could play a bridging role between them because the CDW is associated with each phenomenon. For example, in the LSCO case, the upper critical doping boundary of the CDW phase is strikingly close to the pseudogap critical doping [33,44,45], supporting the close relationship between the CDW and the pseudogap.

In summary, we carried out resistivity and Cu L-edge RSXS measurements on a single crystal of La-based cuprate, $La_{1.87}Sr_{0.13}Cu_{0.99}Fe_{0.01}O_4$. We found new evidence of the PDW in this system. We also found that its emergence is attributed primarily to the CDW stripe rather than the SDW stripe, although the CDW stripe is developed through intertwining with SDW stripes in this system. In particular, the PDW signature starts to appear when the correlation length of the CDW stripe grows over $8a$. These results indicate the critical role of the CDW stripe in the formation of the PDW order in high-T_c cuprates. Moreover, our findings support the possibility that the PDW is ubiquitous in every high-T_c cuprate system.

*Corresponding author.
fujita@imr.tohoku.ac.jp
†Corresponding author.
jslee@slac.stanford.edu

[1] J. G. Bednorz and K. A. Müller, Z. Phys. B **64,** 189 (1986).
[2] E. Fradkin and S. A. Kivelson, Nat. Phys. **8,** 864 (2012).
[3] E. Fradkin, S. A. Kivelson, and J. M. Tranquada, Rev. Mod. Phys. **87,** 457 (2015).
[4] B. Keimer, S. Kivelson, M. Norman, S. Uchida, and J. Zaanen, Nature (London) **518,** 179 (2015).
[5] P. A. Lee, Phys. Rev. X **4,** 031017 (2014).
[6] M. Zelli, C. Kallin, and A. J. Berlinsky, Phys. Rev. B **86,** 104507 (2012).
[7] F. Yu, M. Hirschberger, T. Loew, G. Li, B. J. Lawson, T. Asaba, J. Kemper, T. Liang, J. Porras, G. S. Boebinger, J. Singleton, B. Keimer, L. Li, and N. P. Ong, Proc. Natl. Acad. Sci. U.S.A. **113,** 12667 (2016).
[8] M. R. Norman and J. C. Séamus Davis, Proc. Natl. Acad. Sci. U.S.A. **115,** 5389 (2018).
[9] Q. Li, M. Hücker, G. D. Gu, A. M. Tsvelik, and J. M. Tranquada, Phys. Rev. Lett. **99,** 067001 (2007).
[10] S. Tajima, T. Noda, H. Eisaki, and S. Uchida, Phys. Rev. Lett. **86,** 500 (2001).
[11] A. Himeda, T. Kato, and M. Ogata, Phys. Rev. Lett. **88,** 117001 (2002).
[12] E. Berg, E. Fradkin, E.-A. Kim, S. A. Kivelson, V. Oganesyan, J. M. Tranquada, and S. C. Zhang, Phys. Rev. Lett. **99,** 127003 (2007).
[13] J. M. Tranquada, G. D. Gu, M. Hücker, Q. Jie, H.-J. Kang, R. Klingeler, Q. Li, N. Tristan, J. S. Wen, G. Y. Xu, Z. J. Xu, J. Zhou, and M. v. Zimmermann, Phys. Rev. B **78,** 174529 (2008).
[14] M. Hücker, M. v. Zimmermann, G. D. Gu, Z. J. Xu, J. S. Wen, Guangyong Xu, H. J. Kang, A. Zheludev, and J. M. Tranquada, Phys. Rev. B **83,** 104506 (2011).
[15] P. Abbamonte, A. Rusydi, S. Smadici, G. D. Gu, G. A. Sawatzky, and D. L. Feng, Nat. Phys. **1,** 155 (2005).
[16] C. C. Homes, S. V. Dordevic, G. D. Gu, Q. Li, T. Valla, and J. M. Tranquada, Phys. Rev. Lett. **96,** 257002 (2006).
[17] Y.-J. Kim, G. D. Gu, T. Gog, and D. Casa, Phys. Rev. B **77,** 064520 (2008).
[18] H. Miao, J. Lorenzana, G. Seibold, Y. Y. Peng, A. Amorese, F. Yakhou-Harris, K. Kummer, N. B. Brookes, R. M. Konik, V. Thampy, G. D. Gu, G. Ghiringhelli, L. Braicovich, and M. P. M. Dean, Proc. Natl. Acad. Sci. U.S.A. **114,** 12430 (2017).
[19] S. D. Edkins, A. Kostin, K. Fujita, A. P. Mackenzie, H. Eisaki, S. Uchida, S. Sachdev, M. J. Lawler, E.-A. Kim, J. C. Séamus Davis, and M. H. Hamidian, Science **364,** 976 (2019).
[20] Y. Wang, S. D. Edkins, M. H. Hamidian, J. C. Séamus Davis, E. Fradkin, and S. A. Kivelson, Phys. Rev. B **97,** 174510 (2018).
[21] Z. Dai, Y.-H. Zhang, T. Senthil, and P. A. Lee, Phys. Rev. B **97,** 174511 (2018).
[22] P. Choubey, S. H. Joo, K. Fujita, Z. Du, S. D. Edkins, M. H. Hamidian, H. Eisaki, S. Uchida, A. P. Mackenzie, Jinho Lee, J. C. Séamus Davis, and P. J. Hirschfeld, Proc. Natl. Acad. Sci. U.S.A. **117,** 14805 (2020).
[23] E. H. da Silva Neto, P. Aynajian, A. Frano, R. Comin, E. Schierle, E. Weschke, A. Gyenis, J. Wen, J. Schneeloch, Z. Xu, S. Ono, G. Gu, M. Le Tacon, and A. Yazdani, Science **343,** 393 (2014).
[24] L. Chaix, G. Ghiringhelli, Y. Y. Peng, M. Hashimoto, B. Moritz, K. Kummer, N. B. Brookes, Y. He, S. Chen, S. Ishida, Y. Yoshida, H. Eisaki, M. Salluzzo, L. Braicovich, Z.-X. Shen, T. P. Devereaux, and W.-S. Lee, Nat. Phys. **13,** 952 (2017).
[25] E. Sterpetti, J. Biscaras, A. Erb, and A. Shukla, Nat. Commun. **8,** 2060 (2017).
[26] I. K. Drozdov, I. Pletikosić, C.-K. Kim, K. Fujita, G. D. Gu, J. C. Séamus Davis, P. D. Johnson, I. Božović, and T. Valla, Nat. Commun. **9,** 5210 (2018).
[27] See Supplemental Material at http://link.aps.org/supplemental/10.1103/PhysRevLett.126.167001 for figures supporting the method validation and additional particle reconstructions.
[28] A. J. Achkar, M. Zwiebler, Christopher McMahon, F. He, R. Sutarto, I. Djianto, Z. Hao, M. J. P. Gingras,

M. Hücker, G. D. Gu, A. Revcolevschi, H. Zhang, Y.-J. Kim, J. Geck, and D. G. Hawthorn, Science **351**, 576 (2016).

[29] K. M. Suzuki, T. Adachi, Y. Tanabe, H. Sato, Y. Koike, Risdiana, Y. Ishii, T. Suzuki, and I. Watanabe, Phys. Rev. B **86**, 014522 (2012).

[30] M. Fujita, M. Enoki, and K. Yamada, J. Phys. Chem. Solids **69**, 3167 (2008).

[31] About the transport measurement: Electrical resistivity was measured down to 2.5 K using a standard dc-four-terminal-probe method with a physical property measurement system (PPMS: Quantum Design).

[32] K. Yamada, C. H. Lee, K. Kurahashi, J. Wada, S. Wakimoto, S. Ueki, H. Kimura, Y. Endoh, S. Hosoya, G. Shirane, R. J. Birgeneau, M. Greven, M. A. Kastner, and Y. J. Kim, Phys. Rev. B **57**, 6165 (1998).

[33] J.-J. Wen, H. Huang, S.-J. Lee, H. Jang, J. Knight, Y. S. Lee, M. Fujita, K. M. Suzuki, S. Asano, S. A. Kivelson, C.-C. Kao, and J.-S. Lee, Nat. Commun. **10**, 3269 (2019).

[34] P. M. Lozano, G. D. Gu, J. M. Tranquada, and Qiang Li, Phys. Rev. B **103**, L020502 (2021).

[35] H.-H. Wu, M. Buchholz, C. Trabant, C. F. Chang, A. C. Komarek, F. Heigl, M. v. Zimmermann, M. Cwik, F. Nakamura, M. Braden, and C. Schüßler-Langeheine, Nat. Commun. **3**, 1023 (2012).

[36] V. Thampy, M. P. M. Dean, N. B. Christensen, L. Steinke, Z. Islam, M. Oda, M. Ido, N. Momono, S. B. Wilkins, and J. P. Hill, Phys. Rev. B **90**, 100510(R) (2014).

[37] H. Kimura, H. Matsushita, K. Hirota, Y. Endoh, K. Yamada, G. Shirane, Y. S. Lee, M. A. Kastner, and R. J. Birgeneau, Phys. Rev. B **61**, 14366 (2000).

[38] Z. Du, H. Li, S. H. Joo, E. P. Donoway, J. Lee, J. C. Séamus Davis, G. Gu, P. D. Johnson, and K. Fujita, Nature (London) **580**, 65 (2020).

[39] G. Ghiringhelli, M. Le Tacon, M. Minola, S. Blanco-Canosa, C. Mazzoli, N. B. Brookes, G. M. De Luca, A. Frano, D. G. Hawthorn, F. He, T. Loew, M. Moretti Sala, D. C. Peets, M. Salluzzo, E. Schierle, R. Sutarto, G. A. Sawatzky, E. Weschke, B. Keimer, and L. Braicovich, Science **337**, 821 (2012).

[40] J. Chang, E. Blackburn, A. T. Holmes, N. B. Christensen, J. Larsen, J. Mesot, R. Liang, D. A. Bonn, W. N. Hardy, A. Watenphul, M. v. Zimmermann, E. M. Forgan, and S. M. Hayden, Nat. Phys. **8**, 871 (2012).

[41] S. Gerber, H. Jang, H. Nojiri, S. Matsuzawa, H. Yasumura, D. A. Bonn, R. Liang, W. N. Hardy, Z. Islam, A. Mehta, S. Song, M. Sikorski, D. Stefanescu, Y. Feng, S. A. Kivelson, T. P. Devereaux, Z.-X. Shen, C.-C. Kao, W.-S. Lee, D. Zhu, and J.-S. Lee, Science **350**, 949 (2015).

[42] A. A. Schafgans, A. D. LaForge, S. V. Dordevic, M. M. Qazilbash, W. J. Padilla, K. S. Burch, Z. Q. Li, S. Komiya, Y. Ando, and D. N. Basov, Phys. Rev. Lett. **104**, 157002 (2010).

[43] B. Lake, H. M. Rønnow, N. B. Christensen, G. Aeppli, K. Lefmann, D. F. McMorrow, P. Vorderwisch, P. Smeibidl, N. Mangkorntong, T. Sasagawa, M. Nohara, H. Takagi, and T. E. Mason, Nature (London) **415**, 299 (2002).

[44] S. Badoux, S. A. A. Afshar, B. Michon, A. Ouellet, S. Fortier, D. LeBoeuf, T. P. Croft, C. Lester, S. M. Hayden, H. Takagi, K. Yamada, D. Graf, N. Doiron-Leyraud, and L. Taillefer, Phys. Rev. X **6**, 021004 (2016).

[45] O. Cyr-Choinière, R. Daou, F. Laliberté, C. Collignon, S. Badoux, D. LeBoeuf, J. Chang, B. J. Ramshaw, D. A. Bonn, W. N. Hardy, R. Liang, J.-Q. Yan, J.-G. Cheng, J.-S. Zhou, J. B. Goodenough, S. Pyon, T. Takayama, H. Takagi, N. Doiron-Leyraud, and L. Taillefer, Phys. Rev. B **97**, 064502 (2018).